



Cite this: *Chem. Commun.*, 2025, 61, 5289

Received 22nd January 2025,  
Accepted 6th March 2025

DOI: 10.1039/d5cc00415b

rsc.li/chemcomm

# Electronic pyroelectricity in a supramolecular assembly of an acceptor–donor–acceptor-type ambipolar $\pi$ -system†

Pritam Sadhukhan,<sup>a</sup> Sk Kalimuddin,<sup>b</sup> Aritri Pal,<sup>a</sup> Tuhin Debnath,<sup>b</sup> Swadesh Paul,<sup>a</sup> Shubhankar Barman,<sup>a</sup> Suhrit Ghosh,<sup>a,c</sup> Mintu Mondal<sup>b</sup> and Anuja Datta<sup>a,c</sup>

**Hydrogen-bonded supramolecular assembly of an acceptor–donor–acceptor (ADA)-type ambipolar  $\pi$ -system containing naphthalene-diimide ( $\pi$ -acceptor) and thiophene ( $\pi$ -donor) conjugated chromophores is examined for promising pyroelectric (PY) and photo-PY properties. A maximum PY coefficient of  $\sim 206 \mu\text{C m}^{-2} \text{K}^{-1}$  (at  $T_c$ ) and multifold enhancement after light irradiation is reported. High energy density, power density and scaled efficiency indicate the efficacy of such a nontrivial system for flexible sensors.**

Scavenging energies that are naturally abundant but are mostly wasted (like heat, pressure or vibrations) and converting them into useful electrical energy is of significant importance.<sup>1</sup> In this context, pyroelectric (PY) materials offer widespread applications in sensing, micro-energy harvesting and thermal imaging.<sup>2</sup> The PY effect in general exists in polar dielectric materials and causes variation in internal polarization through external temperature fluctuations to achieve thermal energy to electrical energy conversion. Fundamentally, the PY effect manifests as a temperature-dependent change in the surface charge distribution, which results in PY current generation in the external circuit,  $i_p = pA(\delta T/\delta t)$ , where  $A$  is the area of the measured surface of the material and the PY coefficient  $p$  quantitatively demonstrates the change in spontaneous polarization over temperature variation ( $\delta P_s/\delta T$ ).<sup>3</sup> Figure-of-merits (FOMs) have been determined for PY materials to analyze their relative potentials for various applications, such as  $F_E$  (for

pyroelectric energy harvesting prospects),  $F_V$  (voltage responsivity),  $F_D$  (detectivity) *etc.*, where a high PY coefficient and a low dielectric constant helps to achieve high FOMs (ESI,† Note).<sup>4</sup> Different materials<sup>5</sup> including ferroelectric (FE) ceramics such as lead zirconate titanate  $\text{Pb}(\text{Zr,Ti})\text{O}_3$ , lithium niobate  $\text{LiNbO}_3$ , single-crystals such as  $[\text{FeCo}]$ , and polymers, namely poly(vinylidene fluoride) (PVDF) and PVDF-TrFe,<sup>1</sup> possess significant PY properties (Table S1, ESI†). However, high temperature synthesis in the case of ceramic PYs, device integration difficulties, selective crystallinity, and heavy metals or fluorine containment in standard PY systems are some of the limitations. In this context, organic supramolecular systems deserve significant attention due to their light weight, lack of toxicity, structural flexibility, biocompatibility, and ease of processing.<sup>6,7</sup>

Recently, we have reported prominent ferroelectricity of the H-bonded supramolecular assembly of the ambipolar  $\text{AD}_2\text{A}$  molecule (Fig. 1a), in which a bithiophene donor is conjugated with two electron deficient naphthalene-monoamide acceptors in both arms.<sup>7</sup> Long range helical order through extended H-bonding was found to be the essential structural prerequisite

<sup>a</sup> School of Applied and Interdisciplinary Sciences, Indian Association for the Cultivation of Science, 2A and 2B Raja S. C. Mullick Road, Kolkata-700032, India. E-mail: psusg2@iacs.res.in

<sup>b</sup> School of Physical Sciences, Indian Association for the Cultivation of Science, 2A and 2B Raja S. C. Mullick Road, Kolkata-700032, India. E-mail: sspmm4@iacs.res.in

<sup>c</sup> Technical Research Centre, Indian Association for the Cultivation of Science, 2A and 2B Raja S. C. Mullick Road, Kolkata-700032, India. E-mail: psuad4@iacs.res.in

† Electronic supplementary information (ESI) available: Pyroelectric generator device fabrication, experimental details, and additional figures on pyroelectricity related measurements. See DOI: <https://doi.org/10.1039/d5cc00415b>

‡ These authors contributed equally.

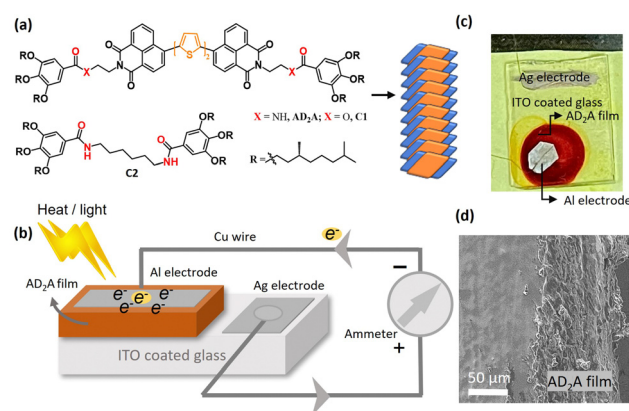


**Fig. 1** (a) Structure of the  $\text{AD}_2\text{A}$  molecule. (b) Schematic diagram of the pyroelectric generator device. (c) Fabricated device. (d) FESEM cross-section image of the  $\text{AD}_2\text{A}$  film.

for the observed room temperature ferroelectricity with pronounced polarization (up to  $2 \mu\text{C cm}^{-2}$ ). It showed a noticeable dielectric anomaly indicating a partial disassembly of the non-covalent assembly at elevated temperatures, which was supported by computational studies and DSC showing disassembly at higher temperature (380 K).<sup>7</sup> These findings motivated us to explore spontaneous polarization driven PY energy harvesting in this AD<sub>2</sub>A system, facilitated by a thermally induced polarization switching. While in most of the conventional PYs, molecular reorientation or displacement is normally utilized to induce polarization switching, AD<sub>2</sub>A chiral molecular assembly employs the partial assembly–disassembly type phase transition to induce polarization change in the absence of an external poling field.<sup>8</sup> In this communication, we have explored the PY and photo-PY properties of the AD<sub>2</sub>A molecule, where the  $P_s$ -driven pyroelectricity could also be triggered by focused light irradiation, essentially a photothermal process, and is seen to be mostly independent of the optical absorption (hence independent of the wavelength of light) of the material.<sup>9</sup> The practical applicability of the designed PY device is predicted from the Olsen cycle, which was adapted to quantitatively determine the maximum energy density as well as power density and scaled efficiency.<sup>10</sup>

Synthesis and supramolecular assembly of AD<sub>2</sub>A was reported by us elsewhere.<sup>7</sup> In brief, it produces a helical fibrillar structure and gelation in hydrocarbon solvents like MCH due to simultaneous H-bonding and  $\pi$ -stacking (Fig. S1, ESI†). A preformed assembly, when transferred to a solid surface, retains its structural features and the internal order as probed in the solution state.<sup>7</sup> The PY generator (Fig. 1b–d) was fabricated using the AD<sub>2</sub>A layer ( $\sim 60 \mu\text{m}$  thick) sandwiched between Ag electrodes and an ITO-coated glass substrate (see ESI,† note for device fabrication). Fig. 2a is the room temperature (rt; 300 K)  $I$ - $V$  characteristic of the fabricated device showing a capacitor type behavior, with low leakage current, confirming good contacts. The PY measurements were carried

out using the Byer–Roundy method (continuous ramping method)<sup>4</sup> in the temperature region between 300 and 380 K. Below 348 K, only a weak current signal is observed upon heating, corresponding to a PY coefficient of less than  $7 \mu\text{C m}^{-2} \text{K}^{-1}$ . As the temperature approaches the Curie temperature, the PY current exhibits a sharp increase, giving a peak as high as  $206 \mu\text{C m}^{-2} \text{K}^{-1}$  at 359 K, and then decreases gradually until 380 K (Fig. 2b). This is clearly associated with the polarization switching, triggered by temperature dependent assembly–disassembly phase transition in the vicinity of the Curie temperature ( $T_c$ ).<sup>11</sup> The integration of current over the temperature domain (300 to 380 K) demonstrates a polarization change of approximately  $2 \mu\text{C cm}^{-2}$  (Fig. 2c). Using our experimental data, the FOM of PY energy harvesting ( $F_E$ ) was calculated to be around  $43.5 \text{ J m}^{-3} \text{K}^{-2}$  near  $T_c$  (Fig. 2d). We consecutively calculated  $F_D$  of  $1.01 \times 10^{-5} \text{ Pa}^{0.5}$ ,  $F_V$  of  $0.11 \text{ m}^2 \text{C}^{-1}$  and voltage coefficient of  $2.22 \times 10^5 \text{ V m}^{-1} \text{K}^{-1}$  at 360 K (Fig. S2, ESI†). Fig. S3 and Table S1 (ESI†) represent the comparison of the PY parameters of AD<sub>2</sub>A with other recently reported organic PY systems, which indicates the superior performance of the AD<sub>2</sub>A supramolecular system. The PY properties of two control molecules C1 and C2 (Fig. 1a) were also investigated. C1 has the same chromophore as that in the AD<sub>2</sub>A; however, the amide groups are replaced by ester groups. In C2, the ambipolar chromophore is absent, though the amide groups are present. In sharp contrast with AD<sub>2</sub>A, both the control systems failed to show any discernible PY current or polarization switching in between 300 and 380 K (Fig. S4, ESI†).

These outcomes unequivocally highlight the distinctive impact of the ambipolar molecular structure as well as its supramolecular assembly, in terms of charge separation and long-range ordering, on the observed commendable pyroelectricity in AD<sub>2</sub>A. In the conventional continuous temperature ramping technique, certain current response resulting from thermally stimulated release of trapped charges may contaminate the PY signal. Therefore, to rule out such possibilities, we have also determined the PY response of the system by thermal oscillation at different background temperatures ranging from rt to the phase transition temperature.<sup>12</sup> In this measurement, such trapped charges are swept out in the primary cycle of temperature modulation and true PY current is selectively detected. Fig. S5 (ESI†) shows the temperature and current for PY measurement upon subjecting the sample to damped temperature of 310 K, 350 K, 360 K and 370 K. While at rt, the thermal oscillation did not produce any significant PY current, at elevated temperatures (350 K and 360 K), noteworthy current release was observed, which was greatly in accordance with the sinusoidal temperature oscillation, with a background temporal modulation in temperature. The appearance of these signals strongly indicates a temperature dependent spontaneous polarization variation due to self-assembly/disassembly alteration in the vicinity of  $T_c$  in the supramolecular AD<sub>2</sub>A system.

The short-circuit current and open-circuit voltage of the AD<sub>2</sub>A film based PY generator is thereby measured by subjecting the sample to a periodic thermal input cycle, upon varying the temperature of the thermal bath from rt to 350 K

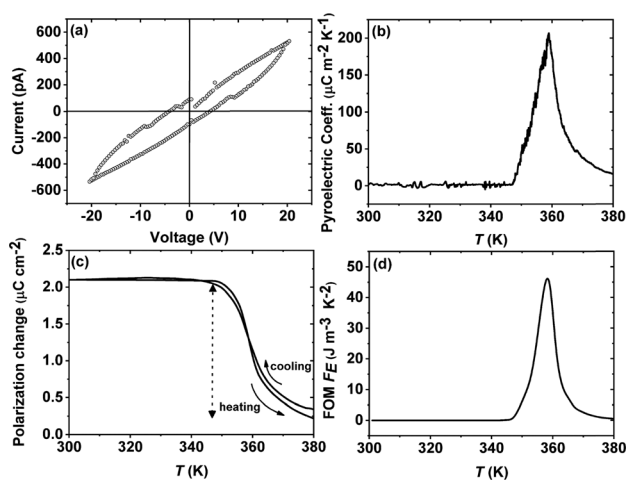


Fig. 2 Pyroelectric (PY) properties of the AD<sub>2</sub>A-film. (a)  $I$ - $V$  characteristics at rt. (b) PY coefficient ( $p$ ) vs.  $T$ . (c) Change in  $P_s$  vs.  $T$ . (d) FOM of energy harvesting ( $F_E$ ).

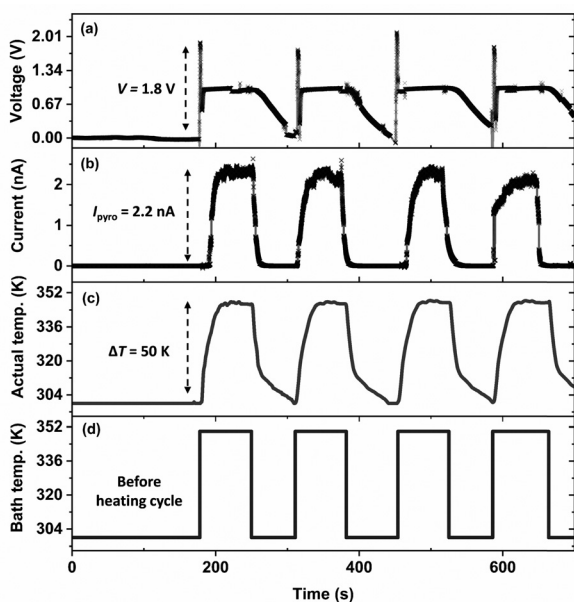


Fig. 3 (a) Open-circuit voltage, (b) short-circuit current. (c and d) Cyclic changes in temperature applied during PY measurements.

(heating 'on' phase) and then down to rt (heating 'off' phase), as shown in Fig. 3a–d and Fig. S6 (ESI<sup>†</sup>).<sup>13</sup> Under forward connection, a sharp positive voltage (up to 1.8 V; Fig. 3a) as well as positive current release (up to 2.2 nA; Fig. 3b) was observed, when the temperature was quickly increased from rt to 350 K ( $\Delta T = 50$  K; Fig. 3c). After a positive voltage/current peak, the current value reached a roughly constant plateau. When the temperature of the sample was kept constant, the current plateau was consistently maintained. This current plateau might have originated as a result of the inbuilt Seebeck effect in the measurement system. The obtained signals changed in sign once the generator device and the measuring system were connected in reverse, indicating that the measured signals were produced due to the switching polarization of the AD<sub>2</sub>A film (Fig. S7, ESI<sup>†</sup>). The stability of the generator was examined by a continuous and constant change of temperature for over 25 cycles and repeated after 45 days (Fig. S8, ESI<sup>†</sup>). Remarkably, the output voltage was stable, indicating steady PY voltage generation. Fig. S9 (ESI<sup>†</sup>) depicts the measured maximum current peak values as a function of temperature change, demonstrating an almost linear relationship. No voltage and current output could be obtained from the control molecules C1 and C2 as anticipated, again corroborating with the claim about the essential role of the molecular and supramolecular design (Fig. S10, ESI<sup>†</sup>).

For the conventional photodetectors, directly exciting photo-carriers with light, beyond the optical bandgap is challenging. On the other hand, a rather instantaneous output current can be produced *via* the photo-PY effect, which can widen the application of a PY material. To check if the photo-PY effect is detectable in the AD<sub>2</sub>A film above rt, laser irradiation (due to focused beam) was chosen for the heat generation on the film surface and the induced PY current is studied in response to

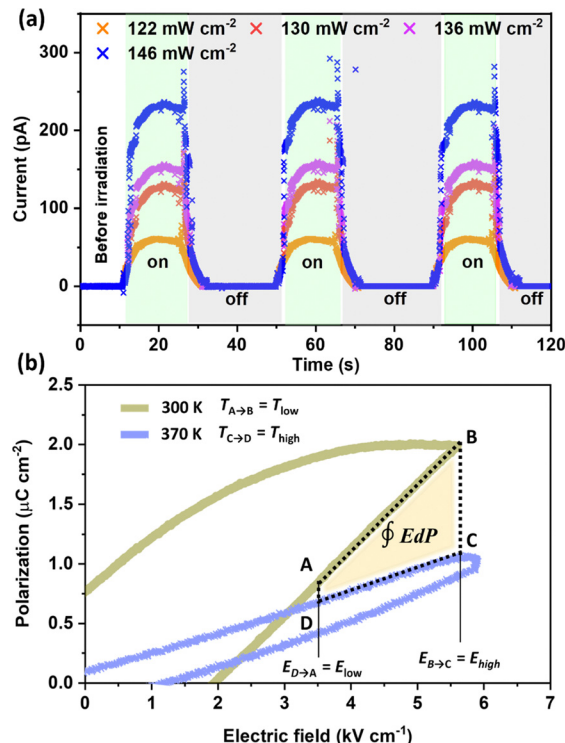


Fig. 4 (a) Photo-response behaviour of the AD<sub>2</sub>A PY device upon light on–off switching, depicting a variation of current intensity as a function of light power density. (b) Olsen cycle performed on the device.

the switching light (on–off–on–off pattern). As shown in Fig. 4a, at 350 K, before the illumination ( $\delta T/\delta t = 0$ ), the supramolecular assembly within the material maintains stability and no spontaneous polarization coupled pyroelectricity is detected. During the laser irradiation ( $\delta T/\delta t > 0$ ), the self-assembly structure within the supramolecular assembly may be partially disordered and that affects the PY response substantially. The repeated order to disordering phenomenon in the supramolecular assembly hence shows a sharp positive transient current spike. *i.e.* light responsive PY current is observed. As the temperature gradually stabilized after a period of laser illumination, the PY current quickly reached a stable plateau, contributing to a stable current arising from the Seebeck effect. When the laser is turned off, the temperature at the surface drops quickly, which induces an equivalent drop in the PY current. The current peaks enlarge significantly with increasing power density of the laser (green laser  $\sim 530$  nm as used here), which can be attributed to the larger polarization alteration in terms of greater temperature fluctuations for higher light intensities (Fig. S11 and Table S2, ESI<sup>†</sup>). The response time of the device thus calculated is shown in Fig. S12 (ESI<sup>†</sup>). This photo-PY current response increases with the increase of the bias voltage, which is due to the enhanced charge separation in this displacive type ferroelectric under higher dc bias as indicated in Fig. S13 (ESI<sup>†</sup>). To further evaluate the self-powered device performance, two key parameters of photoresponsivity ( $R$ ) and detectivity ( $D$ ) are calculated under different light power intensities (ESI, <sup>†</sup> Note).<sup>14</sup> As the power density increases, the PY

current,  $R$  and  $D$  values display an increasing trend, verifying that the photo-PY effect can effectively escalate the photoresponsivity and detectivity (Fig. 4a and Fig. S14, ESI†). Responsivity was also determined with increasing temperature, manifesting higher values in the vicinity of  $T_c$  due to higher PY current (Fig. S15, ESI†).

Having understood the mechanism of the thermal and light induced PY properties of the AD<sub>2</sub>A generator, we also predicted the potential of direct conversion of thermal energy into electrical energy *via* Olsen cycles (Fig. 4b).<sup>10</sup> This cycle is achieved in our PY generator by subjecting the device to time-dependent, spatially uniform temperatures and electric fields. The entire electrical energy density output from the PY cycle is  $1.4 \text{ J L}^{-1}$ , which is represented by the area of the cycle A–B–C–D. Following an initial optimization along the parameters of  $\Delta T = 70 \text{ K}$ ,  $\Delta E = 2.1 \text{ kV cm}^{-1}$  and cycle frequency  $f = 50 \text{ Hz}$ , the energy output parameters yield a maximum power density and scaled efficiency of  $0.093 \text{ W L}^{-1}$  and  $0.25\%$ , respectively, and this data is at par with a number of experimentally investigated organic PY-based energy conversion devices (Table S3 and ESI,† Note). While it is clear that as compared to the commercial crystalline FE polymer, the efficiency is quite low for the AD<sub>2</sub>A, this being the first direct measurement of electronic PY and photo-PY properties in an organic supramolecular assembly system offers the right design and approach for investigating simultaneous thermal and light responsive polarizability in a plethora of other molecular organic systems.

In conclusion, we explored the potential of PY energy harvesting for the first time in a supramolecular assembly of an ADA-type ambipolar FE chromophoric system and revealed the impact of the molecular and supramolecular design on the stimuli responsive polarization switching prospects. The PY generator exhibits a thermo-reversible supramolecular assembly/disassembly in the vicinity of  $T_c$  ( $\sim 360 \text{ K}$ ), with a re-verified polarization change of  $\sim 2 \mu\text{C cm}^{-2}$  and maximum pyroelectric coefficient of  $206 \mu\text{C m}^{-2} \text{ K}^{-1}$ . The maximum open-circuit voltage of  $\sim 1.8 \text{ V}$  and short-circuit current of  $\sim 2.2 \text{ nA}$  were obtained, which was further explored in terms of photo-PY properties and PY Olsen cycles for energy harvesting prospects. Implementation of solid-state pyroelectric Olsen cycles yields a maximum energy density, power density and scaled efficiency of  $1.4 \text{ J L}^{-1}$ ,  $0.093 \text{ W L}^{-1}$  and  $0.25\%$ , respectively. The highlight of this work is in the fine-tuning of the molecular design to facilitate polarization coupled electricity generation in self-poled conditions and through the photonic effect. In contrast to the crystalline and poling dependence optimization in typically reported PVDF and PVDF-TrFe systems, our system is an affordable and sustainable choice for molecular electronics, detectors and pyro photonics applications. Given the simplicity of the molecular design and versatile possibilities of structural variations in the molecular and supramolecular structures of wide-ranging  $\pi$ -systems<sup>15</sup> for organic FE materials, this work

opens up the way for the development of scalable and flexible molecular PYs with comparatively high efficiency and enriched performance.

P. Sadhukhan thanks TRC and the SERB-NPDF (PDF/2023/000786) for the research fellowships. Sk Kalimuddin thanks IACS for a research fellowship. TD thanks UGC for the fellowship. AD and SG thank TRC, IACS for financial support. SG and MM thank IACS for funding.

## Data availability

The data supporting this article have been included as part of the ESI.†

## Conflicts of interest

There are no conflicts to declare.

## Notes and references

- 1 K. Lu, *Materials in Energy Conversion, Harvesting, and Storage*, John Wiley & Sons, Inc., Hoboken, New Jersey, 2014.
- 2 (a) S. B. Lang and S. Muensit, *Appl. Phys. A: Mater. Sci. Process.*, 2006, **85**, 125; (b) H. He, X. Lu, E. Hanc, C. Chen, H. Zhang and L. Lu, *J. Mater. Chem. C*, 2020, **8**, 1494.
- 3 I. Lubomirsky and O. Stafsudd, *Rev. Sci. Instrum.*, 2012, **83**, 051101.
- 4 W. Li, G. Tang, G. Zhang, H. M. Jafri, J. Zhou, D. Liu, Y. Liu, J. Wang, K. Jin, Y. Hu, H. Gu, Z. Wang, J. Hong, H. Huang, L.-Q. Chen, S. Jiang and Q. Wang, *Sci. Adv.*, 2021, **7**, eabe3068.
- 5 (a) Q. Zhang and R. W. Whatmore, *J. Phys. Appl. Phys.*, 2001, **34**, 2296; (b) S. B. Lang, *Phys. Today*, 2005, **58**, 31; (c) P. Sadhukhan, *et al.*, *Nat. Commun.*, 2021, **12**, 4836.
- 6 S. Wang, Y. Bai and T. Zhang, in *Wearable Bioelectronics*, ed. O. Parlak, A. Salleo and A. Turner, Elsevier, 2020, pp. 1–48.
- 7 A. Mukherjee, S. Barman, A. Ghosh, S. Chakraborty, A. Datta, A. Datta and S. Ghosh, *Chem. Sci.*, 2022, **13**, 781.
- 8 M. E. Lines and A. M. Glass, *Principles and applications of ferroelectrics and related materials*, Oxford University Press Inc., New York, 2001.
- 9 J. Tian, *AIP Adv.*, 2023, **13**, 050701.
- 10 S. Pandya, J. Wilbur, J. Kim, R. Gao, A. Dasgupta, C. Dames and L. W. Martin, *Nat. Mater.*, 2018, **17**, 432.
- 11 X. Guan, Z. Lei, R. Xue, Z. Li, P. Li, M. David, J. Yi, B. Jia, H. Huang, X. Li and T. Ma, *Adv. Mater.*, 2024, 2413525.
- 12 B. Bhatia, J. Karthik, T. Tong, D. G. Cahill, L. W. Martin and W. P. King, *J. Appl. Phys.*, 2012, **112**, 104106.
- 13 Y. Yang, W. Guo, K. C. Pradel, G. Zhu, Y. Zhou, Y. Zhang, Y. Hu, L. Lin and Z. L. Wang, *Nano Lett.*, 2012, **12**, 2833.
- 14 X. Zeng, Y. Liu, W. Weng, L. Hua, L. Tang, W. Guo, Y. Chen, T. Yang, H. Xu, J. Luo and Z. Sun, *Nat. Commun.*, 2023, **14**, 5821.
- 15 (a) T. F. A. De Greef, M. M. J. Smulders, M. Wolffs, A. P. H. J. Schenning, R. P. Sijbesma and E. W. Meijer, *Chem. Rev.*, 2009, **109**, 5687; (b) S. S. Babu, V. K. Praveen and A. Ajayaghosh, *Chem. Rev.*, 2014, **114**, 1973; (c) S. Datta, S. Takahashi and S. Yagai, *Acc. Mater. Res.*, 2022, **3**, 259; (d) C. M. Atienza and L. Sánchez, *Chem. – Eur. J.*, 2024, **30**, e202400379; (e) M. Wehner and F. Würthner, *Nat. Rev. Chem.*, 2020, **4**, 38; (f) J. Matern, Y. Dorca, L. Sánchez and G. Fernández, *Angew. Chem., Int. Ed.*, 2019, **58**, 16730; (g) S. Fernández, L. Sánchez, S. S. Babu and G. Fernández, *Angew. Chem., Int. Ed.*, 2024, **63**, e202402259.